EUROfusion

WPMAT-PR(18) 20902

E. Tejado et al.

Determination of R-curves under high temperature by novel elastic method in WCu composites

Preprint of Paper to be submitted for publication in
Materials Science and Engineering A

This work has been carried out within the framework of the EUROfusion Consortium and has received funding from the Euratom research and training programme 2014-2018 under grant agreement No 633053. The views and opinions expressed herein do not necessarily reflect those of the European Commission.

Determination of R-curves under high temperature by novel elastic method in W/Cu composites

E. Tejado[1], A. v. Müller[2,3], J.H. You[2], J.Y. Pastor[1]

[1] Departamento de Ciencia de Materiales-CIME, Universidad Politécnica de Madrid
C/ Profesor Aranguren 3, E28040-Madrid, Spain
[2]Max-Planck-Institut für Plasmaphysik, 85748 Garching, Germany
[3]Technische Universität Munchen, 85748 Garching, Germany

CORRESPONDING AUTHOR:

Elena Tejado
Departamento de Ciencia de Materiales-CIME, Universidad Politécnica de Madrid,
C/ Profesor Aranguren 3, E28040-Madrid, Spain.
Telephone: +34 913 365 243
Email: elena.tejado@upm.es

Abstract

In this work, a model to obtain the crack resistance curve (R-curve) for non-standard samples and with any span-to-depth-ratio has been developed. The use case addresses the three-point-bending fracture of W/Cu metal matrix composites for heat sink applications in future fusion reactors. The model combines the equivalent elastic crack approach to analyse the influence of the properties of the material constituents, i.e. W skeleton with different contents of infiltrated Cu, and the testing environment, high temperature and high vacuum conditions, on the R-curve behaviour. Results showed that W materials exhibit rising R-curve behaviour and that the crack growth resistance is a function of Cu-content and temperature. It is evident, however, that the energy of the high Cu-content samples is higher than that of the low Cu-content samples. Furthermore, the toughening mechanisms and evolution with temperature were identified and assessed.

Keywords: *Tungsten; copper; heat sink; thermo-mechanical properties, fracture mechanics*

1. Introduction

One of the most critical issues to the development of nuclear fusion, as a viable and sustainable source of energy, is the design of structural materials that can withstand the harsh operating conditions inside the reactor. Whilst the experimental reactor ITER is under construction, the final design of the first Demonstration Fusion Power Reactor (DEMO) in Europe is yet to be formally selected [1].

These conditions are especially hostile for the components that line the vacuum vessel and are exposed directly to the plasma (PFM, Plasma Facing Materials) in the divertor. They should work under particularly extreme conditions, both mechanical, thermal and electrical, while subjected to high particle and neutron fluxes. Furthermore, heat fluxes between 1 to 10 MW/m^2 during stationary operation and even up to 20 MW/m^2 in slow transient events are expected in the

divertor region [2]. The heat flux incident on the surface of the PFM must be conducted efficiently through it to the underlying water-cooled heat sink material.

The EU Fusion Programme's 'Materials Assessment Group' (MAG) stablished tungsten as the Baseline Material for state-of-the-art PFC [3], while copper alloys, and especially CuCrZr, are regarded as the materials for the HHF heat sinks in the water-cooled divertor design (monoblock design) due to their superior thermal conductivity, ductility, water-tightness and reduced activation [4] [5]. However, despite these benefits, the main drawback of CuCrZr alloy as structural material for the heat sinks is the rapid loss of ductility under irradiation, which limits the upper temperature for engineering structural applications to 350 °C and for doses up to ~5 dpa.

Furthermore, the integrity of the interface between these baselines materials will be compromised due to the temperature gradient and the difference between the coefficients of thermal expansion and conductivity, 4.2 x 10-6 K-1 and 17.6 x 10-6 K-1 for W and CuCrZ, respectively, thus high stresses are expected at the interface between the PFM and the heat sink material. To overcome these limitations, W/Cu Metal Matrix Composites (MMCs) have been identified as promising candidates for HHF divertor applications, among them, extensive research can be found on fibre and foil reinforced composites [6] [7]. Moreover, the development of a functionally graded material would mitigate thermal stresses in the joint, since thermo-mechanical properties could be tailored just by tailoring the content of each component. In this regard, W/Cu MMCs produced by infiltration of molten copper or copper alloy in a porous W skeleton, whose porosity has been selected earlier, have indeed many advantages [8].

However, notwithstanding promising results on their thermo-mechanical response [9–11], there is still a complete lack of data on both irradiation [12] and reliable fracture toughness values. Even though this latter is considered a key parameter for structural applications. For these reasons, in this work, the influence of both microstructure and temperature on crack propagation of W/Cu composites has been examined. In doing so, a new analytical model has been proposed and implemented for describing the R-curve behaviour.

1.1. Fracture mechanics and its application to the study of cracking of tungsten materials

Fracture toughness of tungsten-based materials is usually studied by means of Linear Elastic Fracture Mechanics (LEFM), due to the brittle nature of W at temperatures below its Ductile to Brittle Transition Temperature (DBTT), but even above it, providing apparent values of the Stress Intensity factor, K_C, for example in [13,14]. This parameter is commonly defined by the expression proposed by Irwin [15]:

$$K = \sigma \sqrt{\pi a}\, F\left(\frac{a}{W}\right) \qquad (0)$$

Where σ is the applied stress and F(a/w) is a geometrical factor that depends on the crack and specimen geometry, a is the crack length, and W is the sample thickness. Fracture toughness, K_{IC}, is then the critical stress intensity factor at the crack tip needed to produce catastrophic failure under simple uniaxial loading (pure Mode I failure).

Thus, strain energy release rate, G, i.e. the energy required to create a new unit crack area, can be written in terms of the crack tip stress intensity factor, K, as [16]:

$$G_c = \frac{K^2}{E'} \qquad (0)$$

Where a is the crack length, σ the applied stress and E' is the generalized elastic modulus (E'=E for plane stress, and E'=E/(1-ν²) for plane strain). The fracture toughness as measured by the critical stress intensity factor K_c and critical strain energy release rate G_c define the resistance of materials against crack growth

However, LEFM is based on the assumption that the material is isotropic and linear elastic, thus the plastic zone ahead of the crack tip should be confined to a narrow region in the fracture process zone. As the plastic zone becomes larger, LEFM breaks down, and plastic deformation has to be considered in detail [17].

When this appends, two parameters are considered for characterizing crack tip toughness of elastic-plastic materials: Crack Tip Opening Displacement (CTOD) suggested by Wells [18], and the J-Integral proposed by Rice [19], and those are intimately related for a given material [20]. Usually, a J-integral based resistance curve (i.e., a J-R curve) is used to describe a ductile material's resistance against crack initiation, stable growth and tearing instability. Stable crack growth results in a continuous fracture toughness versus crack extension, Δa, relationship, the R-curve [21].

The crack extension data may be collected using single-specimen or multiple-specimen techniques. The second procedure involves physical marking of the crack advance, and multiple specimens are used to develop a plot from which a single point initiation toughness value can be evaluated. Nonetheless, it is hard to determine the extent of crack growth accurately because of the diffuse nature of the crack front and the inherent difficulties of the testing environment (achieving testing conditions of temperature and vacuum is extremely time-consuming) and samples itself (millimetric sample sizes). Furthermore, this technique requires the use of at least nine specimens [22], which in the case of high-temperature testing of laboratory-scale materials, is impractical. On the contrary, the single-specimen technique relies on the ability to determine the extent of crack growth while the specimen is loaded in the test frame. Crack growth is determined by an elastic compliance method or by an electrical resistance method, but this latter is restricted because of the limitations of the testing environment. In the elastic compliance technique, rather than letting the test run until the specimen is completely fractured, the sample is unloaded periodically during the test. At each unloading point, Δa is calculated as a function of the slope of the unload line, Young's modulus and specimen geometry. By using this method, the absence of remote yielding can be confirmed, because unloading should result in a return to the origin of the load-displacement diagram. However, due to samples dimensions, it is burdensome to determine the extent of crack growth and therefore a complete fracture is usually achieved.

Consequently, conventional techniques cannot be used in the determination of the crack growth for the materials under study, either by complications associated with the testing environment, i.e. the reduced dimensions of the environmental chamber operating at high temperature and high vacuum atmosphere, or by the early stage of development of these materials, resulting in limited quantities and dimensions of the samples. Therefore, an advanced approach is required for determining the evolution of fracture toughness with temperature and composition, and the micro-mechanisms of failure associated with the process. The following section is devoted to the definition of an elastic equivalent crack through the LEFM and the fundamentals of the compliance method. It was based on the Equivalent Elastic Crack (EEC) approach proposed by Elices and

Planas [23,24], but with the intrinsic benefits that that it is validated for small samples and any span-to-depth ratio.

2. Materials and experimental set-up

2.1. Materials

Three experimental W/Cu MMMCs, corresponding to different content of Cu, were selected for this study. All investigated MMCs were produced in collaboration with Louis Renner GMBH Company (Amtsgericht Stuttgart, Germany) by infiltration of molten Cu in a W skeleton, and later consolidation, at 1150 °C for 2 h, under hydrogen atmosphere. Further details on the production route and prior thermo-mechanical characterization can be found in [25]. Three different compositions were produced with this technique: W-15wt.% Cu, W-30 wt.% Cu and W-40 wt.% Cu. After consolidation, density measurements using the Archimedes method revealed a residual porosity of less than 5 % for both materials. Nomenclature and compositions are listed in Table 1.

2.2. Experimental procedure

For the R-Curve tests, prismatic bars with dimensions 2.8×2.8×30mm^3 were cut using electrical discharge machining (EDM). To facilitate control of crack growth, one side of these specimens was polished down to 1 μm diamond suspension. The specimens were then notched to 2/5 of the height (1.3 mm) using a diamond disc saw with and initial notch radius of 150 μm. Subsequently, a sharper notch was introduced in the bottom of it with a Femto-Second Laser. The final notch radius of all samples yielded between 1-50 nm and laser notches of around 250 μm. Samples were then tested in three-point bending configuration (SELNB), in an INSTRON 8851 universal testing machine (High Wycombe, United Kingdom) with a coupled environmental chamber, and at constant crosshead speed of 100 μm/min. All tests were conducted at room temperature (RT), 425, 550, 675, and 800°C using inductive heating at a heating rate of 10°C/min with 15 min dwell time and under a high vacuum atmosphere (10^{-6} mBar).

2.3. Analytical assessment of the Equivalent Elastic Crack approach for any span-to-depth ratio

In this section the estimation of the EEC approach for the elastic-plastic W/Cu composites under study will be explained in detail.

The output of the fracture tests was recorded as load versus displacement of the frame; this latter was then corrected to remove the system compliance and the uncertainties in the load-displacement curve. Accordingly, the compliance of the sample itself, C_c, can be then written as:

$$C_c = \frac{u}{P} \tag{0}$$

Where P is the applied load and u is its associated thermodynamically conjugate displacement deduced by Planas [26]. In the latter approach, the total compliance, C_c, can be split into the compliance due to the crack existence, $C_c(\alpha)$, and the one of the uncracked specimen C_0. Where α is the crack-to-depth ratio (a/W). Substituting in Eq. (0):

$$C_c(\alpha) = \frac{u}{P} - C_0 \tag{0}$$

C_0 is inferred from the slope of a corrected load–displacement curve, and is calculated as the ratio (du/dP) of specimen displacement to the load carried by the specimen during the test before crack propagates.

Guinea and co-workers [27] deduced a general formula for the crack length as a function of the compliance based on the work by Broek [28]. In it, the relationship between the compliance and the elastic energy contained in the cracked specimen, U, was defined as:

$$U=\frac{1}{2}C_c P^2 \qquad (0)$$

By using the Griffith energy criterion for fracture. The specific energy release rate, G, is then:

$$G=\frac{1}{2}\frac{P^2}{BW}\frac{dC_c}{d\alpha} \qquad (0)$$

Which in terms can be related to the stress intensity factor, K_I, in in Eq. (0), where $G=K_I^2/E'$. Equations (0) and (0) can be then substituted into Eq. (0), and integrated later. So the compliance as a function of α will be:

$$C_c(\alpha)=\frac{1}{E'B}\left[C_1(\alpha)+\beta C_2(\alpha)+\beta^2 C_3(\alpha)\right] \qquad (0)$$

Where β is the span-to-depth ratio, W/L, and the factors $C_1(\alpha)$, $C_2(\alpha)$ and $C_3(\alpha)$ are, respectively:

$$C_1(\alpha)=-0.378\,\alpha^3\ln(1-\alpha)+\alpha^2\frac{0.29+1.39\,\alpha-1.6\,\alpha^2}{1+0.54\,\alpha-0.84\,\alpha^2} \qquad (0)$$

$$C_2(\alpha)=1.1\,\alpha^3\ln(1-\alpha)+\alpha^2\frac{-3.22-16.4\,\alpha+28.1\,\alpha^2-11.4\,\alpha^3}{(1-\alpha)(1+4.7\,\alpha-4\,\alpha^2)} \qquad (0)$$

$$C_3(\alpha)=-0.176\,\alpha^3\ln(1-\alpha)+\alpha^2\frac{8.91-4.88\,\alpha-0.435\,\alpha^2+0.26\,\alpha^3}{(1-\alpha)^2(1+2.9\,\alpha)} \qquad (0)$$

Through this procedure, Guinea et al. deduced the crack length as a function of the compliance by solving numerically Eq. (0) for any value of α:

$$\alpha=\frac{a}{W}=\frac{\left(C_C E' B\right)^{\frac{1}{2}}}{\left[\left(C_C E' B\right)+q_1(\beta)\left(C_C E' B\right)^{\frac{1}{2}}+q_2(\beta)\left(C_C E' B\right)^{\frac{1}{3}}+q_1(\beta)\right]^{\frac{1}{2}}} \qquad (0)$$

Where:

$$q_1(\beta)=0.98+3.77\,\beta \qquad (0)$$

$$q_2(\beta)=\frac{-9.1+2.9\,\beta^2}{1+0.168\,\beta} \qquad (0)$$

$$q_3(\beta)=-3.2\beta+8.9\,\beta^2 \qquad (0)$$

Finally, after substituting the equation (0) for C_c into Eq. (0), we get an expression where the crack length is given with an accuracy better than one percent of the beam depth, W, for any ($C_cE'W$) and for the range of values ($2.5 \le \beta \le 16$). Note that expressions (0) and (0) are only valid for linear elastic materials, thus in the later, we will refer to the equivalent elastic crack, a_{ee}, instead conventional a, when the plastic zone near the crack tip is developed.

The formula for the compliance provides values of a_{ee}, hence α, for every step of the test. Then, the equivalent elastic stress intensity factor, K_{IQee}, may be sought either with Eq. (0) or with the expression proposed by Guinea and coworkers [27] for any span-to-depth ratio, as selected for this work. From it, the R-curve, i.e. the crack extension resistance curve, G_{ee} - Δa_{ee}, can be finally determined.

3. Results and Discussion

3.1. Fracture energy determination

Before the R-curves are calculated, a comparative analysis has been carried out for energy values from two different methodologies. Firstly, LEFM has been used to obtain the values of the critical stress intensity factor, K_{IQ}, as it only brittle behaviour is considered, and the maximum load achieved during the tests. Then, the critical energy release rate, G_{IQ}, defined by Griffiths was estimated from the relationship $G_{IQ}=K_{IQ}^2/E'$. On increasing temperature and copper content, the stress intensity factor loses its validity, thus, apparent values are given here, i.e. sub-index Q.

Secondly, energy values G_F and G_{IC} were obtained with the work-of-fracture method recommended by RILEM [29]. The measured RILEM fracture energy (G_F) represents the average of the local fracture energy function over the ligament area. Once the total work of fracture has been estimated, fracture energy of the materials can be calculated as:

$$G_F=\frac{\int_0^{u_{max}} P\,u_{max}}{b¿¿} \qquad (0)$$

Where the numerator defines the area W_F in . W_F represents the total work of fracture, both elastic and plastic, while the area under the maximum load, W_{IC}, represents the work necessary to create a unit free surface, i.e. the critical energy when cracking starts, thus, it should be in agreement with G_{IQ}.

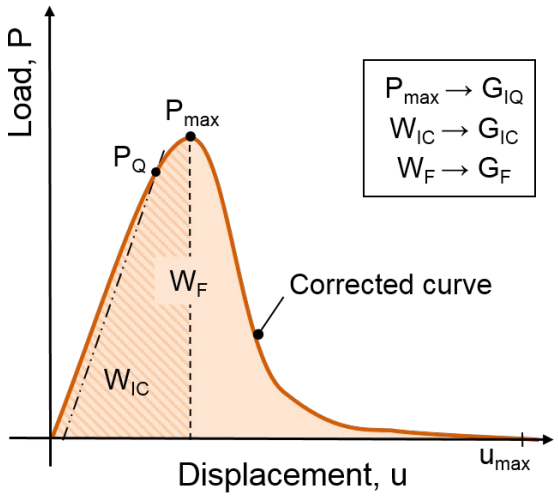

Fig. 1. *Typical load-displacement curve with selected nomenclature for the work-of-fracture method*

Table 1. Fracture energy values for W-Cu compositesTable 1 shows the average values of the fracture energy obtained from the three-point bend tests of W-15Cu, W-30Cu and W-40Cu specimens according to the exposed procedures. The notations used in the table are: the apparent fracture toughness (K_{IQ}) and energy release rate (G_{IQ}) measured with the maximum load (P_{max}) and with the LEFM equations, the RILEM fracture energy (G_F) measured from the total work of fracture (W_F) and the fracture energy (G_{IC}) measured from the work of fracture under maximum load (W_{IC}).

Table 1. *Fracture energy values for W-Cu composites*

Material	*V_{Cu} (wt.%)*	*Temperature (°C)*	*LEFM*		*Work of fracture method (RILEM)*	
			K_{IQ} ($MPa.m^{1/2}$)	*G_{IQ} (kJ/m^2)*	*G_F (kJ/m^2)*	*G_{IC} (kJ/m^2)*
W-15Cu	*15*	*25*	*17.6 ± 0.2*	*1.16 ± 0.03*	*3.1 ± 0.3*	*2.5 ± 0.4*
		300	*19.8 ± 0.8*	*1.6 ± 0.1*	*9.1 ± 0.6*	*2.7 ± 0.2*
		425	*20.0 ± 0.7*	*1.9 ± 0.1*	*19.0 ± 2.0*	*3.0 ± 0.2*
		550	*16 ± 1*	*1.5 ± 0.3*	*10.4 ± 0.2*	*2.3 ± 0.4*
		675	*11.6 ± 0.9*	*1.2 ± 0.2*	*7.2 ± 0.6*	*1.4 ± 0.2*
		800	*10.3 ± 0.6*	*0.9 ± 0.1*	*4.0 ± 0.6*	*1.1 ± 0.1*
W-30Cu	*30*	*25*	*22 ± 0.9*	*2.8 ± 0.2*	*17.9 ± 0.8*	*6.3 ± 0.4*
		300	*21 ± 1*	*2.7 ± 0.3*	*39.8 ± 0.1*	*12 ± 1*
		425	*20 ± 2*	*3.1 ± 0.7*	*39 ± 1*	*9.7 ± 0.8*
		550	*14 ± 2*	*1.5 ± 0.5*	*25 ± 2*	*5.5 ± 0.6*
		675	*11 ± 1*	*1.0 ± 0.3*	*19 ± 3*	*3.9 ± 0.4*
		800	*5.8 ± 0.3*	*0.3 ± 0.1*	*10.9 ± 0.1*	*2.8 ± 0.1*
W-40Cu	*40*	*25*	*18.9 ± 0.3*	*2.6 ± 0.1*	*22.2 ± 1.9*	*6.5 ± 0.3*
		300	*17.7 ± 0.2*	*2.31 ± 0.05*	*47.4 ± 2.3*	*8.3 ± 0.7*
		425	*15.8 ± 0.5*	*1.9 ± 0.1*	*43.8 ± 1.9*	*8.1 ± 0.5*
		550	*11.6 ± 0.1*	*1.06 ± 0.02*	*26.5 ± 0.8*	*5.5 ± 0.5*
		675	*8.1 ± 0.1*	*0.56 ± 0.02*	*19.6 ± 1.8*	*3.7 ± 0.2*
		800	*6.0 ± 0.2*	*0.36 ± 0.02*	*12.4 ± 0.6*	*1.6 ± 0.1*

Apparent values of fracture toughness, K_{IQ}, were already presented in [11] though the procedure followed was insufficient for characterizing the complex fracture behaviour of these composites, a clear trend with temperature was inferred from it, i.e. there was an improvement in the fracture toughness when the Cu content decreases from 40 wt% to 15 wt% (Cu is a weak phase). However, if instead of computing P_Q in the stress intensity factor equation, P_{max} is considered, K_{IQ} and thus, G_{IQ}, are clearly overestimated and no trend can be inferred from them. Consequently, an energy approach other than LEFM should be considered.

Values evaluated experimentally for RILEM fracture energy (G_F) are found to be in reasonable agreement with copper content. When increasing copper content so do the fracture energy released for all the temperature range. The higher values were exhibited by W-40Cu tested between 300 and 425 °C, around 47 and 44 kJ/m^2, respectively. These values are close to the ones observed for W-30Cu at the same temperatures, around 40 kJ/m^2, but much higher than those of W-15Cu composites, 19 kJ/m^2 at 425 °C. The higher values of G_F observed near 400 °C can be related to the DBTT of the tungsten skeleton, which determines the onset of ductile behaviour and shift from a predominantly transgranular cleavage to a intergranular fracture, as observed by Gaganidze [30].

If the materials would exhibit perfect elastic fracture behaviour, values determined experimentally for G_{IC} and G_{IQ} should be equal but since elastic-plastic response was observed, they differ. G_{IC} determines only the elastic energy dissipated in front of notch to propagate till failure whereas G_F gives the total energy dissipated in the beam i.e. to propagate the notch, to create the FPZ in front of notch and possible micro-cracks in beams therefore the difference in value. Furthermore, when a sudden drop in the loading capacity and unstable and fast crack propagation occurs, for example in room temperature tests for low Cu-content materials, the P-u curves are incomplete. In most cases the softening branch in the curves would reveal a positive slope (snap-back behaviour). However, since the controlling parameter was the central deflection instead of a monotonically increasing function of time, i.e. the crack mouth opening displacement, this part of the curve is not registered and the work of fracture method does not provide reliable information.

There is as well an important size-effect, which is commonly observed in fracture toughness and energy measurements of many engineering materials including concrete, fibre reinforced composites and even coarse-grained ceramics. The energy required to create a fresh crack decreases as the crack approaches the free boundary of the specimen, though there is a transition ligament length where the shift from the size-independent fracture energy (G_F) to the rapid decrease occurs. As deduced by Bazant [31], its length depends on the both the material properties and specimen size and shape. Hu and Wittmann [32] argued that the size effect on fracture toughness and energy of a heterogeneous materials will be inevitable if this transition length is less than ten times the initial crack size. These studies essentially recognize that the local fracture energy is not constant over the FPZ. The newly developed methodology allows for this variation as a function of an equivalent elastic crack growth.

3.2. Crack growth resistance curves

Fig. 2 depicts the evolution of G_{ee} with equivalent elastic crack extension at different testing temperatures and for the three composites containing W and Cu, a) W-15Cu, b) W-30Cu and c) W-40Cu, respectively. The load-displacement curves have also been plotted as a function of temperature. Crack growth has been represented up to 1 mm, which corresponds to the 65 % of the initial ligament. Note that for W-15Cu composite tested a RT, linear elastic behaviour up to

fracture is observed. Even though the data acquisition rate was selected to be quite high, 100 Hz, sudden crack growth hinders the fully registration of its development, so a reliable R-curve cannot be obtained.

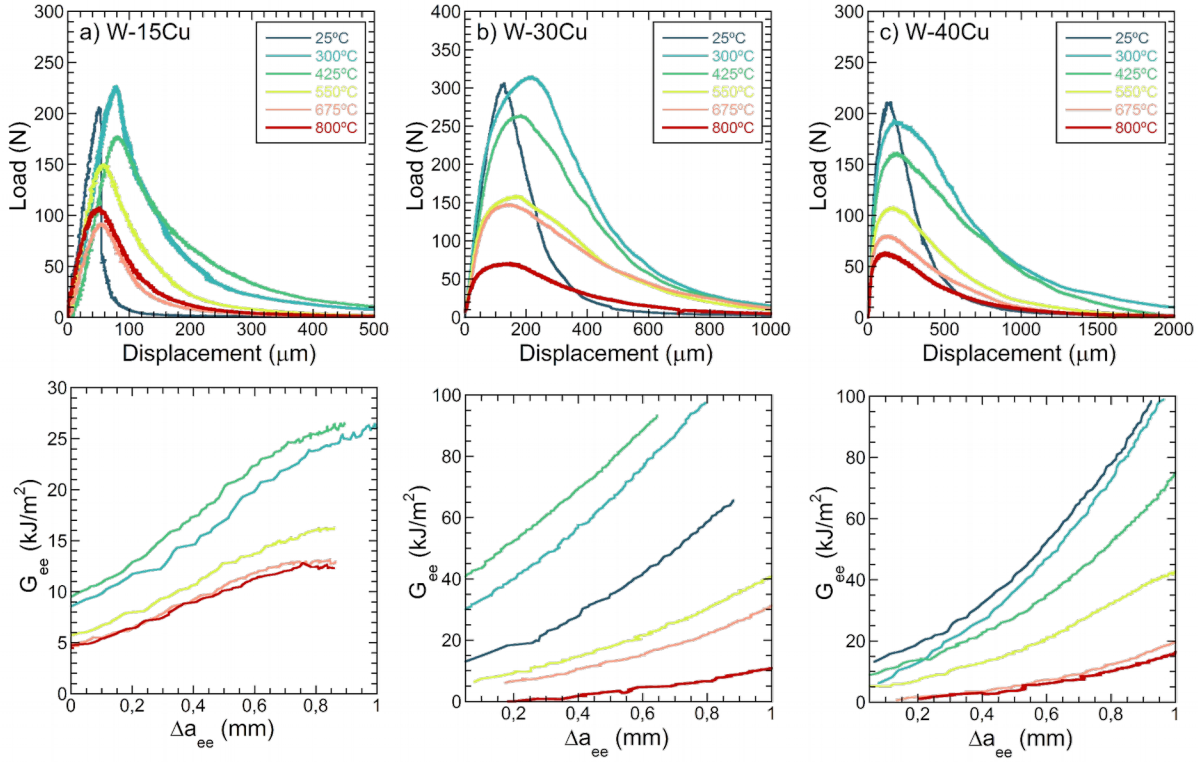

Fig. 2. *Load vs. deflection diagrams and crack growth resistance curves as a function of temperature for a) W-15Cu, b) W-30Cu and c) W-40Cu composites calculated with the EEC approach*

All specimens exhibited a rise in fracture energy with crack extension. It is evident, however, that the energy of the high Cu-content samples is greater than that of the low Cu-content samples. This increase in energy fracture can be quantified by the slope of the resistance curve. W-40Cu composite had a significantly higher growth fracture energy than W-15Cu, while the behaviour of W-30Cu material was intermediate. In addition, the shape of the curves depends as well on the Cu content, shifting from a simple growing curve to a clearly exponential one when its content is the highest.

It should be, however, remarked that at temperatures above 675 °C, the fracture energies exhibited by all the composites are quite low. Up to this temperature, the Cu phase is extremely degraded. Hence, its contribution to the fracture resistance is quite low, and the opposition to the crack growth lies exclusively on the W-phase, which is essentially a foam with 15 to 40 % of pores.

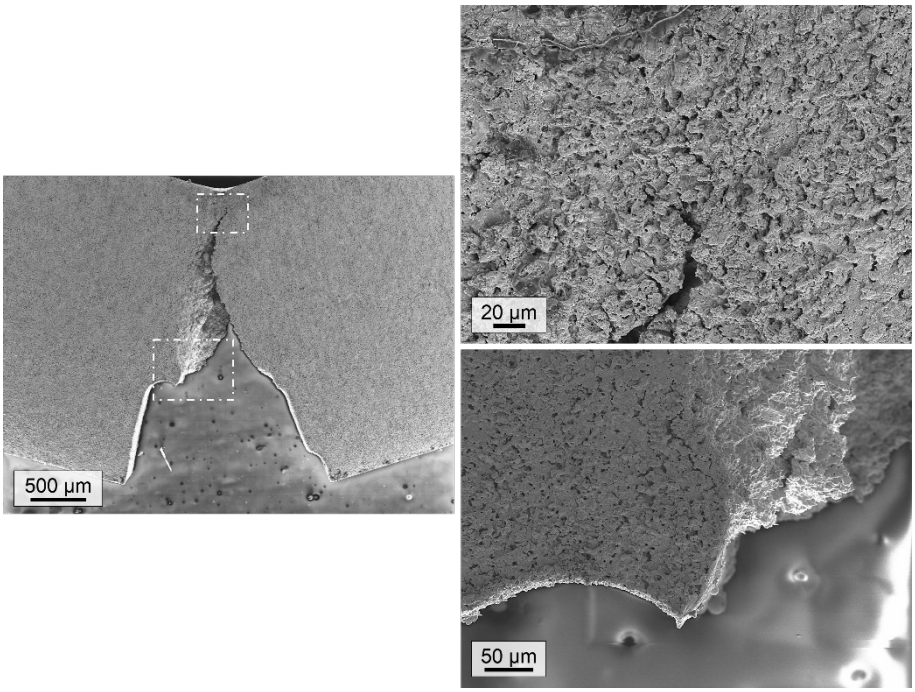

Fig. 3. *SEM micrograph of bridging induced by the copper phase that results in energy dissipation through crack deflection. W-30Cu sample tested at 675 °C*

Furthermore, the variations in energy fracture and therefore, toughness, were correlated to microstructural changes in the crack path, specifically how the crack interacts with the Cu-phase at low temperature and with the preferred fracture mechanisms of pure tungsten at high temperatures. SEM examination of the fracture surfaces, showed evidence of bridging induced by the copper phase residing between the W skeleton. The fracture surfaces exhibited broken ligaments spread across the specimen thickness (Fig. 3 and Fig. 4), as well as complex crack growth patterns in the W skeleton. Notice that the crack propagates through two distinct zones with unique morphologies. The first one is the W skeleton characterised by a continuous straight path of transgranular fracture especially at low temperatures (Fig. 5 a), whereas the second zone, the Cu phase, exhibits a discontinuous path with evidence of crack deflection, crack bifurcation, and many fractured ligaments that bridged the crack. Therefore, crack growth in the composites was frequently arrested by the ductile copper phase and required higher driving forces to continue extension, as higher is the content of copper, higher is the energy required to break the un-cracked region.

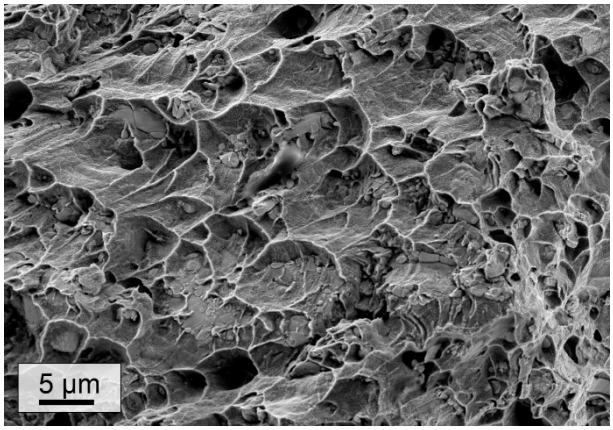

Fig. 4. *SEM micrograph of bridging induced by the tearing of the Cu phase in a W-40Cu specimen tested at 425 °C. Extensive Cu deformation results in Cu ligaments and energy dissipation*

Analogous to features observed with different copper contents, the SEM observation of the fracture surfaces revealed a transition from rough surface in the W skeleton of the samples tested at low temperatures to a smooth fracture plane in the samples tested at higher temperatures. When its DBTT is overcome, shifting from a transgranular fracture below the DBTT to an intergranular fracture over it, as depicted in the above schemes (Fig. 5). These two behaviours were distinctly evident; thus, it can be established that the crack growth resistance is a function of temperature and copper content.

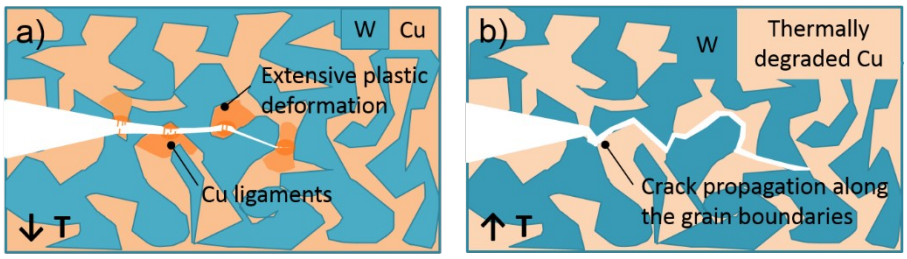

Fig. 5. *Schematic diagrams of crack propagation. a) At low temperatures (T<500 °C), Cu phase causes local crack deflection and results in the formation of bridges in the crack wake, while generating an extensive plastic deformation that inhibits the crack growth. Transgranular fracture is predominant in W phase. b) At high temperatures (T<500 °C), degradation of Cu phase lower the energy dissipation while predominant intergranular fracture of W phase is observed.*

Two fracture surfaces of W-15Cu composite tested at low (25 °C) and high (675 °C) temperatures are presented in Fig. 6. At 25 °C the fracture surface shows clear cleavage; the energy is absorbed before crack propagation, not during crack propagation. At higher temperatures, the energy necessary to promote intergranular fracture decreases, so this mechanism is preferred for the crack advance. This change could be related to nature of the dislocation substructures observed in tungsten by Stephens in the late sixties [33], at temperatures greater than 0.1 Tm, the dislocation structures in the refractory metals are characterised predominantly by edge dislocations, while up to that temperature, screw dislocations characterise the structures.

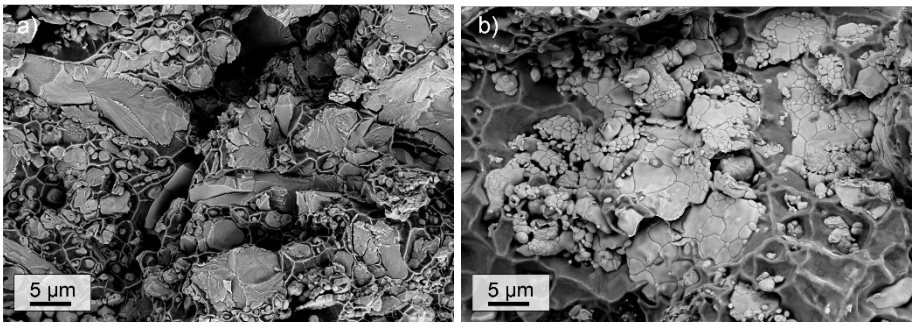

Fig. 6. *SEM micrographs of fracture surfaces of W-15Cu specimens tested at a) 25 °C and b) 675 °C under a vacuum atmosphere. The change in the fracture mode of the W skeleton can be observed: at low temperatures crack propagation is predominantly transgranular whereas intergranular fracture is observed at high temperatures*

4. Conclusions

An elastic equivalent crack has been defined through the LEFM and the fundamentals of the compliance method. The main objective was the investigation of the fracture mechanical properties of novel W-Cu metal matrix composites.

Several issues, regarding sample sizes and results obtained, should be considered for linear elastic fracture mechanics to be applied. It is necessary that the plastic zone, i.e. the FPZ, near the crack tip has a small size as compared to the sample dimensions. These should be large enough to meet

the requirements of the standards and to provide a size-independent fracture property. However, labscale materials do not meet these demands, furthermore, the size of the final component in the reactor will be, in some cases, on the scale of the testing specimens.

In the view of the limitations, an elastic-plastic fracture theory approach instead of LEFM should be made. Thus, the ductile fracture should be defined with crack growth resistance curves. However, as exposed previously, the limitations of sample sizes, composition (very brittle material combined with a very ductile metal) and the testing environment make the proper measurement of the crack advance an arduous task. To solve this, a new method has been developed.

An equivalent elastic crack has been proposed with an approximation of the EEC model proposed by Elices (Elices & Planas 1993) and the compliance methods, but with the unique singularity that it can be used with small samples and with any span-to-depth ratio. The model was applied to calculate the R-curves of the W-Cu composites. Energies related to the process were also evaluated with the Griffiths and RILEM equations. However, local fracture energy is not constant over the FPZ so this variation should be accounted with the fracture energy curves.

For the first time, R-curves of W based composites have been obtained. Results showed that W materials exhibit rising R-curve behaviour and that the crack growth resistance is a function of Cu-content and temperature. It is evident, however, that the energy of the high Cu-content samples is higher than that of the low Cu-content samples. This increase in energy fracture can be quantified by the slope of the resistance curve. W-40Cu composite had a significantly higher growth fracture energy than W-15Cu, while the behaviour of W-30Cu material was intermediate.

4. Acknowledgements

This work has been carried out within the framework of the EUROfusion Consortium and has received funding from the EURATOM research and training programme 2014-2018 under grant agreement No 633053. The views and opinions expressed herein do not necessarily reflect those of the European Commission.

The authors also acknowledge the support of the Ministerio de Economía y Competitividad of Spain (research project MAT2015-70780-C4-4-P) and the Comunidad de Madrid (research project S2013/MIT-2862-MULTIMATCHALLENGE) who have funded this research.

References

[1] G. Federici, C. Bachmann, W. Biel, L. Boccaccini, F. Cismondi, S. Ciattaglia, M. Coleman, C. Day, E. Diegele, T. Franke, M. Grattarola, H. Hurzlmeier, A. Loving, F. Maviglia, B. Meszaros, C. Morlock, M. Rieth, M. Shannon, N. Taylor, M.Q. Tran, J.H. You, R. Wenninger, L. Zani, Overview of the design approach and prioritization of R&D activities towards an EU DEMO, Fusion Eng. Des. 109–111 (2016) 1464–1474.

[2] J.H. You, E. Visca, C. Bachmann, T. Barrett, F. Crescenzi, M. Fursdon, H. Greuner, D. Guilhem, P. Languille, M. Li, S. McIntosh, A.V. Müller, J. Reiser, M. Richou, M. Rieth, European DEMO divertor target: Operational requirements and material-design interface, Nucl. Mater. Energy. 9 (2016) 171–176.

[3] D. Stork, P. Agostini, J.L. Boutard, D. Buckthorpe, E. Diegele, S.L. Dudarev, C. English, G. Federici, M.R. Gilbert, S. Gonzalez, A. Ibarra, C. Linsmeier, A. Li Puma, G. Marbach, P.F. Morris, L.W. Packer, B. Raj, M. Rieth, M.Q. Tran, D.J. Ward, S.J. Zinkle, Developing structural, high-heat flux and plasma facing materials for a near-term DEMO fusion power plant: The EU assessment, J. Nucl. Mater. 455 (2014) 277–291.

[4] S.A. Fabritsiev, S.J. Zinkle, B.N. Singh, Evaluation of copper alloys for fusion reactor divertor and first wall components, J. Nucl. Mater. 233–237 (1996) 127–137.

[5] J.H. You, Copper matrix composites as heat sink materials for water-cooled divertor target, Nucl. Mater. Energy. 5 (2015) 7–18.

[6] A. Herrmann, H. Greuner, M. Balden, H. Bolt, Design and evaluation of an optimized W/Cu interlayer for W monoblock components, Fusion Eng. Des. 86 (2010) 27–32.

[7] H. Greuner, A. Zivelonghi, B. Böswirth, J.H. You, Results of high heat flux testing of W/CuCrZr multilayer composites with percolating microstructure for plasma-facing components, Fusion Eng. Des. 98–99 (2015) 1310–1313.

[8] J.-H.H. You, A. Brendel, S. Nawka, T. Schubert, B. Kieback, Thermal and mechanical properties of infiltrated W/CuCrZr composite materials for functionally graded heat sink application, J. Nucl. Mater. 438 (2013) 1–6.

[9] A. V Müller, D. Ewert, A. Galatanu, M. Milwich, R. Neu, J.Y. Pastor, U. Siefken, E. Tejado, J.H. You, Melt infiltrated tungsten–copper composites as advanced heat sink materials for plasma facing components of future nuclear fusion devices, Fusion Eng. Des. 124 (2017) 455–459.

[10] E. Tejado, A. v. Müller, J.-H. You, J.Y. Pastor, Evolution of mechanical performance with temperature of W/Cu and W/CuCrZr composites for fusion heat sink applications, Mater. Sci. Eng. A. 712C (2018) 738–746.

[11] E. Tejado, A. V Müller, J.-H. You, J.Y. Pastor, The thermo-mechanical behaviour of W-Cu metal matrix composites for fusion heat sink applications: The influence of the Cu content, J. Nucl. Mater. 498 (2018) 468–475.

[12] D. Stork, P. Agostini, J.-L. Boutard, D. Buckthorpe, E. Diegele, S.L. Dudarev, C. English, G. Federici, M.R. Gilbert, S. Gonzalez, A. Ibarra, C. Linsmeier, A.L. Puma, G. Marbach, L.W. Packer, B. Raj, M. Rieth, M.Q. Tran, D.J. Ward, S.J. Zinkle, Materials R&D for a timely DEMO: Key findings and recommendations of the EU Roadmap Materials Assessment Group, Fusion Eng. Des. 89 (2014) 1586–1594.

[13] E. Tejado, P.A. Carvalho, A. Muñoz, M. Dias, J.B. Correia, U.V. Mardolcar, J.Y. Pastor, The effects of tantalum addition on the microtexture and mechanical behaviour of tungsten for ITER applications, J. Nucl. Mater. 467 (2015).

[14] T. Palacios, J.Y. Pastor, M.V. Aguirre, M.A. Monge, R. Pareja, Mechanical Behaviour of Tungsten-Vanadium-Lanthana Alloys as Function of temperature, J. Nucl. Mater. (2013).

[15] G.R. Irwin, Analysis of Stresses and Strains Near the End of a Crack Traversing a Plate, J. Appl. Mech. 24 (1957) 361–364.

[16] A.A. Griffith, The Phenomena of Rupture and Flow in Solids, Philos. Trans. R. Soc. London A Math. Phys. Eng. Sci. 221 (1921).

[17] B. Cotterell, The past, present, and future of fracture mechanics, Eng. Fract. Mech. 69 (2002) 533–553.

[18] A. Wells, Application of fracture mechanics at and beyond general yielding, 10 (1963) 563–70.

[19] J.R. Rice, A path independent integral and the approximate analysis of strain concentration by notches and cracks, J. Appl. Mech. 35 (1968) 379–86.

[20] C.F. Shih, Relationships between the J-integral and the crack opening displacement for stationary and extending cracks, J. Mech. Phys. Solids. 29 (1981) 305–326.

[21] X.-K.K. Zhu, J.A. Joyce, Review of fracture toughness (G, K, J, CTOD, CTOA) testing and standardization, Eng. Fract. Mech. 85 (2012) 1–46.

[22] ASM International., Characterization and failure analysis of plastics., ASM International, 2003.

[23] M. Elices, J. Planas, Equivalent elastic crack. 1: Load-Y equivalences, Kluwer Academic Publishers, 1993.

[24] J. Planas, M. Elices, G. Ruiz, The equivalent elastic crack: 2. X-Y equivalences and asymptotic analysis, Int. J. Fract. 61 (1993) 231–246.

[25] A.V. Muller, D. Ewert, A. Galatanu, M. Milwich, R. Neu, J.Y. Pastor, U. Siefken, E. Tejado, J.H. You, Melt infiltrated tungsten–copper composites as advanced heat sink materials for plasma facing components of future nuclear fusion devices, Fusion Eng. Des. 124 (2017).

[26] J. Planas, G. V. Guinea, M. Elices, Stiffness associated with quasi-concentrated loads, Mater. Struct. 27 (1994) 311–318.

[27] G. V. Guinea, J.Y. Pastor, J. Planas, M. Elices, Stress Intensity factor, compliance and CMOD for a General Three-Point-Bend Beam, Int. J. Fract. 89 (1998) 103–116.

[28] D. Broek, Elementary engineering fracture mechanics, Springer Netherlands, Dordrecht, 1982.

[29] RILEM TCS, Determination of the fracture energy of mortar and concrete by means of three-point bend tests on notched beams, Mater. Struct. 18 (1985) 287–290.

[30] E. Gaganidze, D. Rupp, J. Aktaa, Fracture behaviour of polycrystalline tungsten, J. Nucl. Mater. 446 (2014) 240–245.

[31] Z.P. Bazant, J. Planas, Fracture and Size E↗ect in Concrete and Other Quasibrittle Materials, in: CRC Press, Boca Ratón, Florida, 1998.

[32] X. Hu, F. Wittmann, Size effect on toughness induced by crack close to free surface, Eng. Fract. Mech. 65 (2000) 209–221.

[33] J.R. Stephens, NASA Technical Note: Dislocation structures in single crystal tungsten and tungsten alloys, Whashington D.C., 1969.